Zero-Point Fluctuations in Naphthalene and Their Effect on Charge Transport Parameters

Joe J. Kwiatkowski,* Jarvist M. Frost, James Kirkpatrick, and Jenny Nelson

Department of Physics, Imperial College, London, SW7 2AZ, U.K.

Received: May 22, 2008; Revised Manuscript Received: July 10, 2008

We calculate the effect of vibronic coupling on the charge transport parameters in crystalline naphthalene, between 0 and 400 K. We find that nuclear fluctuations can cause large changes in both the energy of a charge on a molecule and on the electronic coupling between molecules. As a result, nuclear fluctuations cause wide distributions of both energies and couplings. We show that these distributions have a small temperature dependence and that, even at high temperatures, vibronic coupling is dominated by the effect of zero-point fluctuations. Because of the importance of zero-point fluctuations, we find that the distributions of energies and couplings have substantial width, even at 0 K. Furthermore, vibronic coupling with high energy modes may be significant, even though these modes are never thermally activated. Our results have implications for the temperature dependence of charge mobilities in organic semiconductors.

1. Introduction

Despite the huge interest in the electronic applications of conjugated organic solids, there remain fundamental questions to be answered about the exact mechanism of charge transport in these materials. The description of charge transport is complicated by the disorder that is intrinsic to these materials and by the effect of this disorder on charge transport parameters. Disorder in organic solids may arise from impurities[1] or from the noncrystalline packing of molecules.[2] However, even in a perfect crystal, disorder can be caused by nuclear vibrations which also change the value of charge transport parameters. The effect of nuclear fluctuations on the electronic charge transport parameters is known as vibronic coupling. We quantify the effect of vibronic coupling on charge transport parameters in crystalline naphthalene and investigate its temperature dependence.

Within the tight-binding approximation, charge transport through a molecular solid can be described by the Hamiltonian,[3]

$$\mathscr{H} = \sum_i \varepsilon_i(\underline{\xi}) a_i^\dagger a_i + \sum_{ij} J_{ij}(\underline{\xi}) a_i^\dagger a_j \qquad (1)$$

The site energy ε_i is the energy of a charge on molecule i. This charge is created and annihilated by operators $a_i^\dagger$ and a_i, respectively. J_{ij} is the electronic coupling between molecules i and j. Both ε_i and J_{ij} are a function of nuclear coordinates $\underline{\xi}$.

Using a Hamiltonian similar to eq 1, Troisi et al. have proposed a model for charge transport that correctly predicts the temperature dependence of the charge mobility in pentacene.[4] Pentacene displays "bandlike" transport, where the charge mobility decreases with increasing temperature because thermal nuclear fluctuations increasingly interfere with charge transfer. Troisi et al. predict the correct temperature dependence by taking large distributions of ε_i and J_{ij} that increase with temperature.

The importance of vibronic coupling has previously been shown.[5,3,6,7] In particular, it has been demonstrated that nuclear fluctuations cause wide distributions of J_{ij} between pentacene molecules.[8] However, to our knowledge, the effect of nuclear fluctuations on ε_i has not been rigorously investigated in conjugated organic solids. Furthermore, studies of vibronic coupling to date have always treated nuclear vibrations as classical and therefore their results are limited to high temperatures.

We quantify the effect of vibronic coupling on J_{ij} and ε_i over a temperature range from 0 to 400 K. To do so, we use both quantum and classical sampling methods. In order to permit large sampling sets and to allow the use of computationally expensive quantum chemical calculations, we work with naphthalene instead of pentacene. We simply consider the two molecules in the naphthalene unit cell. For hole transport, the electronic coupling between highest occupied molecular orbitals (HOMOs) of the two uncharged molecules is relevant; we denote this as J_{HOMO}. For electron transport, the relevant coupling is between the lowest unoccupied molecular orbitals (LUMOs), denoted J_{LUMO}. Likewise, the site energies for holes and electrons are $\varepsilon_{\mathrm{HOMO}}$ and $\varepsilon_{\mathrm{LUMO}}$, respectively. Because we only consider a single unit cell, and because the site energy of molecule i depends on the entire surrounding lattice, we are unable to determine the absolute value of $\varepsilon^i_{\mathrm{HOMO}}$. Instead, we calculate the difference in site energies for hole transport,

$$\Delta\varepsilon_{\mathrm{HOMO}} = \varepsilon_{\mathrm{HOMO}}{}^2 - \varepsilon_{\mathrm{HOMO}}{}^1 \qquad (2)$$

Molecules 1 and 2 are shown in Figure 1.

2. Methodology

We consider the effect of nuclear fluctuations on J_{HOMO}, J_{LUMO}, and $\Delta\varepsilon_{\mathrm{HOMO}}$ for the two molecules in the $P2_1/a$ unit cell of naphthalene, shown in Figure 1. We find that density functional theory (DFT) methods are required to accurately calculate the effect of intramolecular vibrations on electronic structure. All electronic calculations (Imperial College High Performance Computing Service; URL: http:// www.imperial.ac.uk/ict/services/teachingandresearchservices/highperformancecomputing) are therefore performed with DFT in the generalized gradient approximation of PW91[9] and the 6-311G* basis set with tight convergence criteria as implemented in Gaussian.[10] The methods used to calculate J and $\Delta\varepsilon$ are given in ref 11 and are not discussed further here.

The atomic coordinates of each molecule are optimized with DFT and their relative positioning is taken from an experimental

* Corresponding author. E-mail: joek@cantab.net.

10.1021/jp8045406 CCC: $40.75
Published on Web 08/28/2008

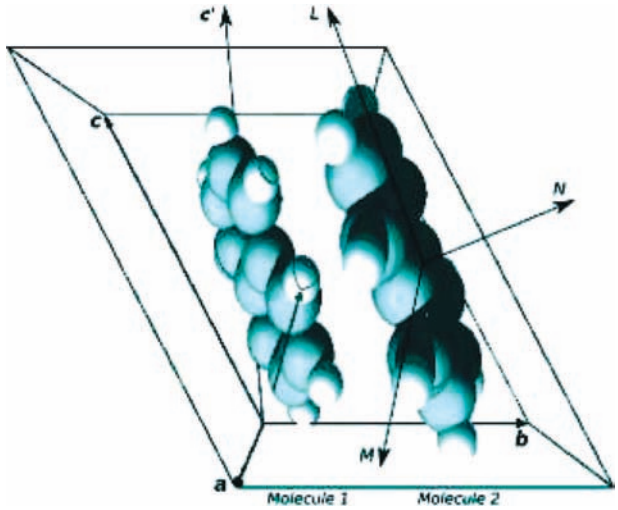

Figure 1. $P2_1/a$ unit cell of naphthalene showing the lattice vectors and axes of phonon librations.

structure.[12] The value of J_{HOMO} that is calculated for the undistorted molecules is found to be in good agreement with similar results in the literature.[3] In order to sample the vibronic coupling over a wide range of temperatures, we use both quantum and classical methods to sample nuclear fluctuations.

2.1. Quantum Sampling. Our quantum sampling method relies upon the harmonic approximation. A distortion from the optimized geometry of the two molecules $\Delta\underline{\xi}$ is described by a superposition of distortions along the normal modes of the system $\underline{\chi}_q$ so that $\Delta\underline{\xi} = \xi_1\underline{\chi}_1 + \xi_2\underline{\chi}_2 + \cdots + \xi_{3N-3}\underline{\chi}_{3N-3}$. If the normal modes are considered to be independent and harmonic, the Hamiltonian of the system is given by

$$\mathcal{H} = \sum_{q=1}^{3N-3}\left(-\frac{\hbar^2}{2\mu_q}\frac{\partial^2}{\partial\xi_q^{\,2}} + \frac{1}{2}\mu_q\omega_q^{\,2}\xi_q^{\,2}\right) \tag{3}$$

where the energy of the optimized geometry has been set to zero. The three translations of the entire unit cell are ignored since these modes are irrelevant to the interaction between the two molecules in the cell. μ_q is the reduced mass of mode q, and ω_q is its frequency. When in equilibrium with a thermal bath of temperature T, the probability of a distortion ξ_q along mode q is given by[13]

$$p_q(\xi_q, T) = \sqrt{\frac{m_q\omega_q^{\,2}}{2\pi E_q^{\mathrm{th}}}}\exp\left(-\frac{m_q\omega_q^{\,2}\xi_q^{\,2}}{2E_q^{\mathrm{th}}}\right) \tag{4}$$

where E_q^{th} is the thermal energy of mode q given by $E_q^{\mathrm{th}} = (n_q^{\mathrm{th}} + {}^1/_2)\hbar\omega_q$. The average number of excited quanta in the oscillator, n_q^{th}, is given by the Bose−Einstein distribution. The probability of distortion $\Delta\underline{\xi}$ is given by

$$p(\Delta\underline{\xi}, T) = \prod_q^{3N-3} p_q(\xi_q, T) \tag{5}$$

It is worth stressing that at absolute zero $E_q^{\mathrm{th}}(0\ \mathrm{K}) = {}^1/_2\hbar\omega_q$, and as a result, there remains a finite probability of distortion $\Delta\underline{\xi}$ away from the equilibrium geometry.

The accuracy of this sampling method relies on the accuracy of the harmonic approximation. As temperatures rise, molecular distortions become larger and higher order terms in eq 3 become non-negligible, so the approximation breaks down. Previous studies on biphenyl have demonstrated that quantum sampling can be accurate up to several hundred kelvin.[14] We assess the validity of the harmonic approximation in section 3.1.

TABLE 1: Frequencies and Reduced Masses of the Nine Optical Phonon Modes of Crystalline Naphthalene[a]

mode		Γ-point frequency (cm^{-1})	reduced mass (amu)
translations:	**a**	106.74	7.11
	b	78.05	7.11
	c′	57.71	7.11
in-phase librations:	L	130.09	4.12
	M	54.37	5.21
	N	84.06	4.85
out-of-phase librations:	L	112.41	4.12
	M	64.38	5.21
	N	79.39	4.85

[a] Frequencies are taken from ref 17. See Figure 1 for description of modes.

We assume that the intermolecular phonon modes are uncoupled to the intramolecular vibrational modes. This has been shown to be a reasonable approximation for naphthalene.[15] The intramolecular modes, their frequencies, and reduced masses are calculated with high precision frequency calculations and agree well with the literature.[16] As discussed above, we neglect the acoustic phonons since we are only dealing with molecules within a single unit cell. For the optical phonon modes, we take the frequencies from the Γ point of neutron scattering experiments.[17] The reduced masses of the optical modes are calculated as the renormalization factor in the transformation from Cartesian to mass-weighted coordinates, consistent with the treatment of the intramolecular modes. Table 1 summarizes the details of the optical phonon modes that we used in our sampling.

2.2. Classical Sampling. We use the MM3 forcefield[18] which is fitted to structural and vibrational data for hydrocarbon crystals.[19] By calculating the bond order of sp^2 carbons semiempirically, MM3 predicts a structure for naphthalene that is in good agreement with experiment.[20]

We simulate a supercell of naphthalene composed of $4 \times 4 \times 4$ primitive unit cells whose structure was taken from ref 12. Periodic boundary conditions were applied in all directions. The supercell was relaxed into the MM3 energy minimum with a tolerance of 1.0 kcal/(mol Å); though this changes the bond lengths slightly, it is an essential step to avoid structural stress which would otherwise disturb the initial dynamics of the simulation. All calculations were done with the TINKER package.[21,22]

Dynamic simulations were carried out at 100, 200, 300, and 400 K in an *NPT* ensemble at atmospheric pressure with Berendsen's algorithm[23] and timesteps of 1 fs. Coordinate snapshots were taken every 10 ps over a total simulation time of 1 ns; we assume that 10 ps is long enough to ensure that there is no correlation between snapshots. In order to preserve a large range of normal mode components, only C−H bond lengths were constrained. The geometry of molecules in each unit cell were taken from each of these snapshots and these coordinates were used to perform the single point quantum chemical calculations discussed above.

Classically sampling distortions along normal mode q with frequency ω_q is only valid if $\hbar\omega_q$ is substantially smaller than k_BT where k_B is Boltzmann's constant. Therefore classical sampling will perform badly at low temperatures or where high frequency modes are important.

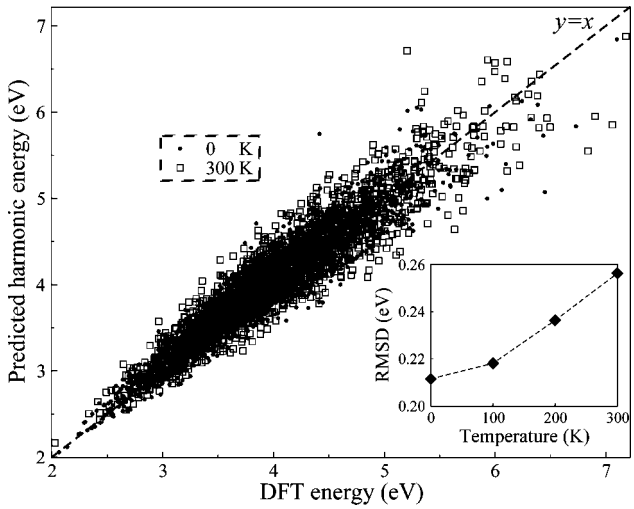

Figure 2. Potential energy of distortion as predicted by the harmonic approximation and as calculated with DFT at 0 and 300 K. The inset shows the root-mean-square deviation between harmonic and DFT energies as a function of temperature.

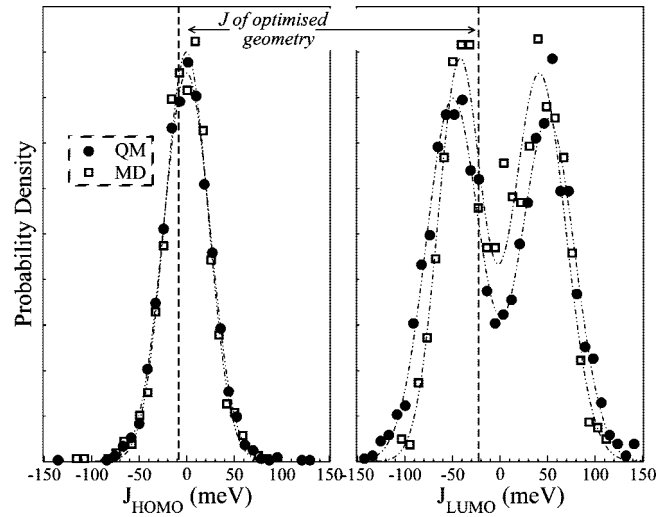

Figure 3. Distribution of the J_{HOMO} and J_{LUMO} at 200 K: classical (molecular dynamics (MD)) and quantum (quantum mechanics (QM)) sampling of molecular configurations.

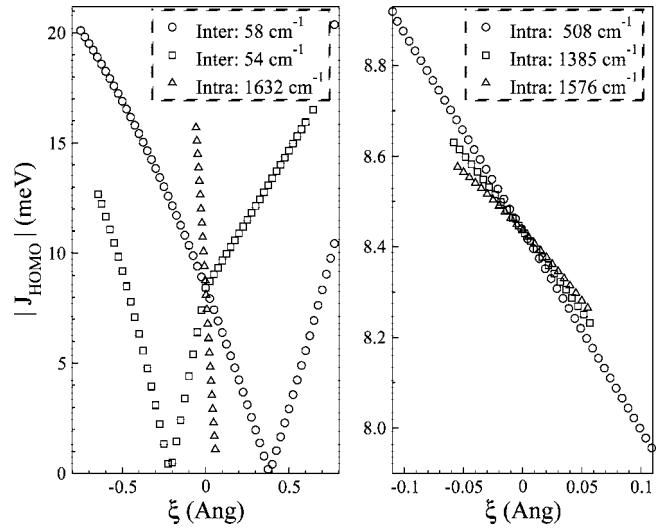

Figure 4. Variation in $|J_{HOMO}|$ for distortions of a single molecule along a single mode. A range of intermolecular and intramolecular modes are shown—note the large difference in the scales of the two graphs. Distortions are sampled to $\xi_q(T) = (2E_q^{th}(T)/k_q)^{1/2}$ at 300 K.

3. Results

Except where stated, the quantum sampling method used 2000 points while the classical method used 1000 points; in both cases, we found this was sufficient for good convergence.

3.1. Harmonic Approximation. We first assess the accuracy of our quantum sampling method by testing the harmonic approximation (eq 3). Figure 2 shows the correlation between the potential energies as predicted by the harmonic approximation and as calculated by DFT. Even at 0 K the harmonic values are not perfectly correlated to the DFT values, perhaps because distortions along different modes are not perfectly additive or because the harmonic approximation is already inaccurate for some modes. As expected, the harmonic approximation is worse at 300 K because the distortions along each normal mode are larger so that higher order terms in eq 3 become important. The root-mean-square deviation between harmonic and the DFT energies as a function of temperature is shown as an inset to Figure 2. Since the average potential energy of a distortion at 0 K is almost 4 eV, a disagreement between harmonic and DFT energies of 0.2 eV can be regarded as small. The harmonic approximation appears valid even at 300 K, perhaps because naphthalene is a relatively stiff molecule with only a few low energy vibrational modes.

3.2. Distribution of *J*. Figure 3 shows the distribution of J_{HOMO} and J_{LUMO} at 200 K, with molecular configurations sampled by both classical and quantum methods. We find that the spread in J is very large compared to its typical magnitude, a result which agrees with a similar study of pentacene.[8]

The results from classical and quantum sampling are very similar. This suggests that the low frequency intermolecular phonon modes are largely responsible for modulating J and that, at 200 K, these modes are accurately sampled by both quantum and classical methods.

Figure 4 plots the change in the absolute HOMO coupling $|J_{HOMO}|$ as molecule 2 is distorted along a single mode while molecule 1 is kept in its optimized geometry. All other modes are frozen. Distortions along several intermolecular and intramolecular modes are shown up to the point where $\xi_q(T) = (2E_q^{th}/k_q)^{1/2}$ at 300 K; classically, this is equivalent to the maximum distortion of the harmonic oscillator at 300 K. Note that for the high energy intermolecular modes, $\xi_q(0\text{ K}) \simeq \xi_q(300\text{ K})$ because $n_q^{th} \simeq 0$ in both cases. Large distortions up to 0.8 Å are possible along the low energy modes and these can vary $|J_{HOMO}|$ by over 20 meV. This is consistent with results in ref 24. Because distortions are smaller along the high energy modes, they generally have a smaller effect on $|J_{HOMO}|$. However, the mode at 1632 cm^{-1} is an exception to this rule and has a very large effect on $|J_{HOMO}|$. The vibronic coupling of individual modes is discussed in more detail in section 3.4.

3.3. Distribution of $\Delta\varepsilon$. Figure 5 shows the distribution of $\Delta\varepsilon_{HOMO}$ at 200 K as sampled by classical and quantum methods. $\Delta\varepsilon_{HOMO}$ is the energy required by holes to transfer from molecule 1 to molecule 2; the fact that $\Delta\varepsilon_{HOMO}$ is usually large and positive implies that molecule 1 is generally energetically favored by holes (see Figure 1). This is because a hole in the HOMO of molecule 2 interacts unfavorably with the positively charged hydrogens of molecule 1.[11] However, nuclear fluctuations can occasionally shift the energetic balance to favor molecule 2.

The agreement between classical and quantum sampling is poor. This is because high energy modes are important, and these are not sampled accurately with the classical method; this

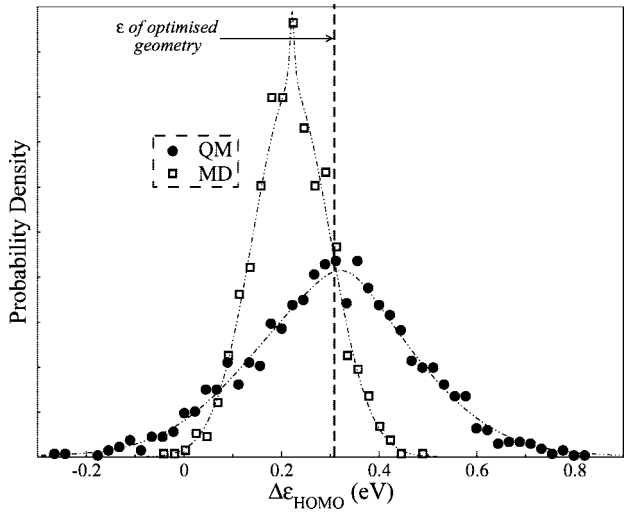

Figure 5. Distribution of $\Delta\varepsilon_{HOMO}$ at 200 K: classical (MD) and quantum (QM) sampling of molecular configurations.

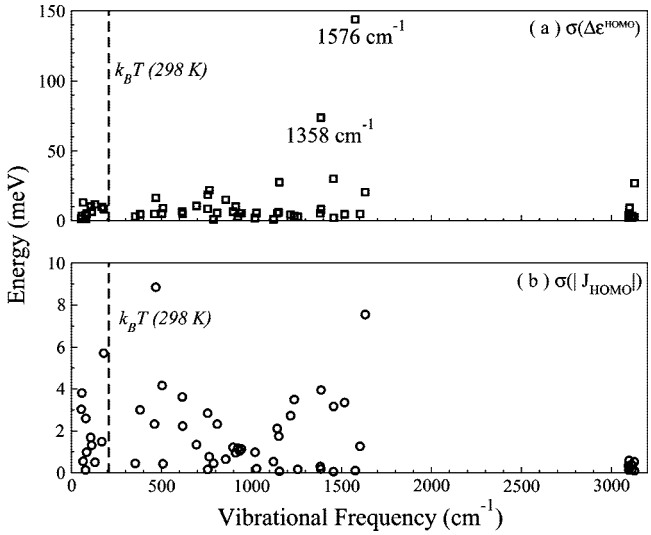

Figure 6. Standard deviation of (a) $\Delta\varepsilon_{HOMO}$ and (b) $|J_{HOMO}|$ due to distortions along individual modes at 0 K: quantum sampling of molecular configurations.

is discussed further in section 3.4. Our distributions of $\Delta\varepsilon_{HOMO}$ are consistent with studies on one-dimensional intermolecular distortions of pentacene pairs.[11]

3.4. Effect of Zero-Point Fluctuations. We calculate the vibronic coupling of zero-point fluctuations along a single normal mode by freezing all other modes, sampling distortions along the chosen mode at 0 K, and measuring the standard deviation in $\Delta\varepsilon_{HOMO}$ and $|J_{HOMO}|$. Both molecules are allowed to distort independently along the chosen mode. For each mode we sample 100 distortions.

The standard deviations $\sigma(|J_{HOMO}|)$ and $\sigma(\Delta\varepsilon_{HOMO})$ are shown in Figure 6 against the vibrational frequency of each mode. This figure shows that zero-point fluctuations can be responsible for large values of $\sigma(|J_{HOMO}|)$ and $\sigma(\Delta\varepsilon_{HOMO})$.

Although it is commonly known that low energy modes can modulate J_{HOMO} significantly,[6,11] Figure 6 demonstrates that high energy modes can also have significant effects. While never thermally activated, small distortions along high energy modes can nevertheless give $\sigma(|J_{HOMO}|)$ of about 4 meV. This is a significant modulation in $|J_{HOMO}|$ as it is half the value of $|J_{HOMO}|$ in the optimized geometry of the two molecules.

As suggested in section 3.3, $\Delta\varepsilon_{HOMO}$ is particularly sensitive to distortions along high energy modes. Modes at 1385 and 1576 cm^{-1} modulate $\Delta\varepsilon_{HOMO}$ very strongly indeed. These modes symmetrically stretch the C−C bonds which are defined by the HOMO. Therefore even small distortions along these modes substantially change the energy of the HOMO and so ε_{HOMO}.

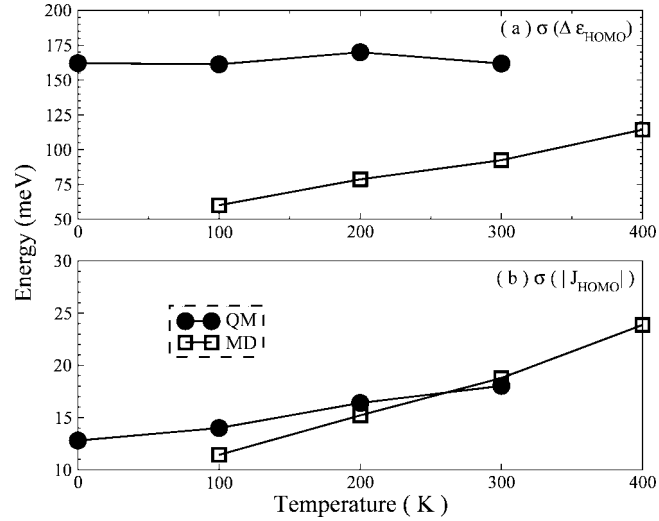

Figure 7. Effect of temperature on the standard deviation of (a) $\Delta\varepsilon_{HOMO}$ and (b) $|J_{HOMO}|$ distributions: classical (MD) and quantum (QM) sampling of molecular configurations.

Because a range of modes contribute to the deviation in both $\Delta\varepsilon_{HOMO}$ and J_{HOMO}, the electronic structure of organic solids must fluctuate over a wide range of timescales, from the period of the slowest intermolecular mode (∼650 fs) to the period of the fastest intramolecular mode (∼10 fs). The modulation of J by high energy modes has possible implications for the Franck−Condon approximation that is made in semiclassical Marcus theory and this is discussed in the Supporting Information.

3.5. Temperature Dependence of Vibronic Coupling. Figure 7 shows the temperature dependence of $\sigma(|J_{HOMO}|)$ and $\sigma(\Delta\varepsilon_{HOMO})$ as sampled with both classical and quantum methods. Because of the effect of zero-point fluctuations, we find that there is substantial disorder in both J_{HOMO} and $\Delta\varepsilon_{HOMO}$ at 0 K.

Because the effect of low energy modes dominate $\sigma(|J_{HOMO}|)$ at high temperatures, there is good agreement between classical and quantum methods, as discussed in section 3.2. However, even at 300 K, $\sigma(|J_{HOMO}|)$ is only 1.4 times larger than the deviation at 0 K. This implies that although the low energy modes are thermally activated, their contribution to the total vibronic coupling is dominated by distortions that would happen anyway at 0 K. Because of the importance of the zero-point fluctuations, the classical sampling method underestimates the value of $\sigma(|J_{HOMO}|)$ at low temperatures and overestimates its temperature dependence.

Because $\Delta\varepsilon_{HOMO}$ is almost entirely modulated by the zero-point fluctuations of high energy modes (section 3.4), and because these modes are never thermally activated in this temperature range, $\sigma(\Delta\varepsilon_{HOMO})$ is independent of temperature. Because of its inability to treat the zero-point fluctuations of these modes, the classical method drastically underestimates $\sigma(\Delta\varepsilon_{HOMO})$ and incorrectly predicts a temperature dependence.

We suggest these results are relevant to charge transport in ultra pure organic crystals. Charge transport in these crystals is described as "bandlike" because the charge mobility is limited by thermal fluctuations.[25] The mobility therefore shows a negative temperature dependence and its largest value is at

temperatures that tend to 0 K. Recent work has explained the bandlike transport in pentacene in terms of $\sigma(|J_{HOMO}|)$ and $\sigma(\Delta\varepsilon_{HOMO})$ that increase with temperature.[4] Our results show that the temperature dependence of $\sigma(|J_{HOMO}|)$ and $\sigma(\Delta\varepsilon_{HOMO})$ is not as large as would be predicted by a purely classical approach, and this will have implications on the temperature dependence of the charge mobility. Furthermore, our results suggest that the largest possible charge mobility at 0 K will be limited by the effect of nuclear zero-point fluctuations on $\sigma(|J_{HOMO}|)$ and $\sigma(\Delta\varepsilon_{HOMO})$.

4. Conclusions

We have illustrated that a consideration of vibronic coupling is important for an accurate description of intermolecular charge transfer in conjugated organic solids. We have shown that substantial spreads in the values of J and $\Delta\varepsilon$ can be caused by zero-point fluctuations and that high energy modes, which may never be thermally activated, can nevertheless have substantial effects. We have demonstrated that the effects of zero-point fluctuations dominate vibronic coupling, even at temperatures as high as 300 K. When the effects of zero-point fluctuations are properly considered, the vibronic coupling has a temperature dependence that is smaller than would be predicted by purely classical methods; this has implications on the temperature dependence of charge mobility in organic semiconductors with bandlike charge transport. We suggest that the largest charge mobilities possible in these materials (at 0 K) will be determined by the effect of zero-point fluctuations on $\sigma(|J_{HOMO}|)$ and $\sigma(\Delta\varepsilon_{HOMO})$.

Acknowledgment. We would like to thank Dr. Patricia Hunt (Imperial College London) for her helpful comments.

Supporting Information Available: Discussion of the Franck−Condon approximation that is made in semiclassical Marcus theory. Though not necessarily applicable to naphthalene, semiclassical Marcus theory is commonly used to describe charge transfer between conjugated organic molecules. The Franck−Condon approximation allows J_{ij} to be treated as a constant throughout the charge transfer; we analyze this approximation for naphthalene based on our above results. This material is available free of charge via the Internet at http://pubs.acs.org.

References and Notes

(1) Forrest, S. R. *Nature* **2004**, *428*, 911–918.
(2) Kwiatkowski, J. J.; Nelson, J.; Li, H.; Bredas, J. L.; Wenzel, W.; Lennartz, C. *PCCP* **2008**, *10* (14), 1852–1858.
(3) Coropceanu, V.; Cornil, J.; da Silva, D. A.; Olivier, Y.; Silbey, R.; Bredas, J. L. *Chem. Rev.* **2007**, *107* (5), 2165–2165.
(4) Troisi, A.; Orlandi, G. *Phys. Rev. Lett.* **2006**, *96* (8), xx.
(5) Sanchez-Carrera, R. S.; Coropceanu, V.; da Silva Filho, D. A.; Friedlein, R.; Osikowicz, W.; Suess, R. C.; Salaneck, W. R.; Bredas, J. L. *J. Phys. Chem. B* **2006**, *110*, 18904–18911.
(6) Lemaur, V.; Da Silva Filho, D.; Coropceanu, V.; Lehmann, M.; Geerts, Y.; Piris, J.; Debije, M.; Van de Craats, A.; Senthilkumar, K.; Siebbeles, L.; Warman, J.; Bredas, J.; Cornil, J. *J. Am. Chem. Soc.* **2004**, *126* (10), 3271–3279.
(7) Wang, L. J.; Peng, Q.; Li, Q. K.; Shuai, Z. *J. Chem. Phys.* **2007**, *127*, 044506.
(8) Troisi, A.; Orlandi, G. *J. Phys. Chem. A* **2006**, *110* (11), 4065–4070.
(9) Perdew, J. P.; Chevary, J. A.; Vosko, S. H.; Jackson, K. A.; Perderson, M. R.; Singh, D. J.; Fiolhais, C. *Phys. Rev. B* **1992**, *46* (11), 6671–6687.
(10) Frisch, M. J.; Trucks, G. W.; Schlegel, H. B.; Robb, M. A.; Cheeseman, J. R.; Montgomery, J. A.; Kudin, K. N.; Burant, J. C.; Millam, J. M.; Barone, V.; Mennucci, B.; Cossi, M.; Petersson, G. A.; Nakatsuji, H.; Hada, M.; Fukuda, R.; Hasegawa, J.; Ishida, M.; Nakai, H.; Klene, M.; Li, X.; Adamo, C.; Jaramillo, J.; Gomperts, R.; Austin, A. J.; Cammi, R.; Pomelli, C.; Morokuma, K.; Voth, G. A.; Salvador, P.; Zakrzewski, V. G.; Dapprich, S.; Daniels, A. D.; Farkas, O.; Malick, D. K.; Rabuck, A. D.; Foresman, J. B.; Ortiz, J. V.; Cui, Q.; Cioslowski, J.; Stefanov, B. B.; Liu, G.; Komaromi, I.; Martin, R. L.; Fox, D. J.; Peng, C. Y.; Nanayakkara, A.; Challacombe, M.; Johnson, B.; Chen, W.; Wong, M. W. *Gaussian 03*, revision B.05; Gaussian Inc.: Pittsburgh PA, 2003.
(11) Valeev, E. F.; Coropceanu, V.; da Silva, D. A.; Salman, S.; Bredas, J. L. *J. Am. Chem. Soc.* **2006**, *128* (30), 9882–9886.
(12) Ponomarev, V. I.; Filipenko, O. S.; Atovmyan, L. O. *Kristallografiya* **1976**, *21* (2), 392–394.
(13) Feynmann, R. P. *Statistical Mechanics: A Set of Lectures*; Perseus: Cambridge, MA, 1998.
(14) Pecchia, A.; Gheorghe, M.; Di Carlo, A.; Lugli, P.; Niehaus, T.; Frauenheim, T.; Scholz, R. *Phys. Rev. B* **2003**, *68* (23), xx.
(15) Pawley, G. S.; Cyvin, S. J. *J. Chem. Phys.* **1970**, *52*, 4073.
(16) Kato, T.; Yamabe, T. *J. Chem. Phys.* **2001**, *115* (18), 8592.
(17) Natkaniec, I.; Bokhenkov, E. L.; Dorner, B.; Kalus, J.; MacKenzie, G. A.; Pawley, G. S.; Schmelzer, U.; Sheka, E. F. *J. Phys. C: Solid State Phys.* **1980**, *13* (23), 4265–4283.
(18) Allinger, N. L.; Yuh, Y. H.; Lii, J.-H. *J. Am. Chem. Soc.* **1989**, *111* (23), 8551–8566.
(19) Lii, J.-H.; Allinger, N. L. *J. Am. Chem. Soc.* **1989**, *111* (23), 8566–8575.
(20) Allinger, N. L.; Li, F.; Yan, L.; Tai, J. C. *J. Comput. Chem.* **1990**, *11* (7), 868–895.
(21) Kundrot, C. E.; Ponder, J. W.; Richards, F. M. *J. Comput. Chem.* **1991**, *12* (3), 402–409.
(22) Dudek, M. J.; Ponder, J. W. *J. Comput. Chem.* **1995**, *16* (7), 791.
(23) Berendsen, H. J. C.; Postma, J. P. M.; van Gunsteren, W. F.; DiNola, A.; Haak, J. R. *J. Chem. Phys.* **1984**, *81*, 3684.
(24) Bredas, J.; Beljonne, D.; Coropceanu, V.; Cornil, J. *Chem. Rev.* **2004**, *104* (11), 4971–5003.
(25) Warta, W.; Stehle, R.; Karl, N. *Appl. Phys. A: Mater. Sci. Process.* **1985**, *36* (3), 163–170.

JP8045406